



Feasibility of active handheld NDVI sensors for monitoring lichen ground cover

R. Erlandsson^{a,*}, M.K. Arneberg^a, H. Tømmervik^a, E.A. Finne^{a,b}, L. Nilsen^c, J.W. Bjerke^a

^a Norwegian Institute for Nature Research, High North Research Centre for Climate and the Environment, Box 6606 Langnes, NO-9296, Tromsø, Norway

^b Department of Geosciences, University of Oslo, NO-0316, Oslo, Norway

^c UiT, The Arctic University of Norway, N-9019, Tromsø, Norway

ARTICLE INFO

Corresponding Editor: Peter Crittenden

Keywords:

Lichen
Pale lichens
Cladonia
NDVI
Active sensor
Remote sensing
Monitoring

ABSTRACT

Vegetation indices are corner stones in vegetation monitoring. However, previous field studies on lichens and NDVI have been based on passive sensors. Active handheld sensors, with their own light sources, enables high-precision monitoring under variable ambient conditions. We investigated the use of handheld sensor NDVI for monitoring pale lichen cover across three study sites from boreal heathlands to High Arctic tundra (62–79 °N), and compared it with Sentinel-2 satellite NDVI. NDVI decreased with increasing cover of pale lichens but the correlation between active and satellite NDVI varied between areas. NDVI values declined with lichen cover and ranged from 0.4–0.18 when lichen cover was above 40%. Active ground measurements of NDVI explained 81% of the variation in the satellite NDVI values in Svalbard (High Arctic), while the relationships were lower (~30% explained variation) in boreal regions (Troms-Finnmark and Røros). We show that active sensors are feasible for extracting information from lichen-dominated vegetation.

1. Introduction

Lichens are a diverse group of fungi with photosymbionts that are adapted to grow in all climates and on all substrates – from leaves of evergreen trees via asphalt and other manmade substrates to polar soils and rocks. Terricolous lichens, i.e. lichens that grow on soil and rocks, constitute an important landcover type with global distribution. They are particularly abundant in non-forested and non-agricultural regions of the world (e.g., tundra, drylands, heaths, and fog oases). In cool climates, erect (fruticose) mat-forming lichens are able to outcompete vascular plants and bryophytes, especially on nutrient-poor sandy soils, resulting in vast areas at high latitudes and altitudes dominated by lichens.

Species of the pale lichen genus *Cladonia* are commonly known as reindeer lichens since they are an important forage resource for reindeer and caribou (*Rangifer*) (Brodo et al., 2001; Joly et al., 2009; Tømmervik et al., 2012). Recently, increased grazing from *Rangifer* due to larger populations, especially semi-domesticated, has led to steep declines in lichen biomass and reduced ground cover of lichen-dominated vegetation in both Eurasia and North America (Joly et al., 2009; Fraser et al., 2014; Kumpula et al., 2014; Sandström et al., 2016). In addition, the increasing impacts of climate change will put additional pressure on

terricolous lichens by favouring the establishment of vascular plants in areas traditionally dominated by lichens (Fraser et al., 2014). The mechanisms behind those changes are not strictly a direct effect of increasing temperatures per se, as lichens typically tolerate high temperatures, but rather a shift in abiotic conditions, like dew, that favour vascular plants (Proctor 2012). Since global warming is amplified at higher latitudes (Serreze and Barry 2011; Blunden and Boyer 2021), rapid and pronounced changes in lichen distribution and abundance may be expected at high latitudes in the near future (Joly et al., 2009; Fraser et al., 2014; Chagnon et al., 2021).

Remote sensing is a vital tool for monitoring and quantifying large-scale vegetation changes (Piao et al., 2020). However, in contrast to green plants, efficient methods for remote sensing of lichens have been quite elusive (Nordberg and Allard 2002; Rees et al., 2004; Kennedy et al., 2020). Yet, the Normalised Difference Vegetation Index (NDVI), which is closely positively correlated with green biomass, and therefore has been used for crop and vegetation monitoring for over 40 years (Rouse et al., 1974; Tucker 1979; Myneni et al., 1997) was one of the most important predictors of lichen biomass in an artificial intelligence based remote sensing method recently developed by Erlandsson et al. (2022). In earlier studies NDVI has been shown to be negatively correlated with increasing lichen cover (Solheim 1998; Nordberg and Allard

* Corresponding author. Norwegian Institute for Nature Research, High North Research Centre for Climate and the Environment, NO-9296, Tromsø, Norway.

E-mail address: rasmus.erlandsson@nina.no (R. Erlandsson).

<https://doi.org/10.1016/j.funeco.2023.101233>

Received 20 May 2022; Received in revised form 29 January 2023; Accepted 6 February 2023

Available online 4 March 2023

1754-5048/© 2023 The Authors. Published by Elsevier Ltd. This is an open access article under the CC BY license (<http://creativecommons.org/licenses/by/4.0/>).

2002). Presently, however, nearly all field-based studies on NDVI from lichen-rich sites have been based on traditional, *passive* sensors that rely on the reflectance of sunlight (e.g., Bokhorst et al., 2012; Edwards and Henry 2016) or portable field spectrometers that monitor a wide range of wavelengths (ca. 325–1075 nm), from which the wavelengths used to calculate NDVI can be retrieved (e.g. Gamon et al., 2013). Although undeniably useful, passive sensors are sensitive to light conditions, solar angle, haze and shadows, while portable field spectrometers are costly and require some post-processing to retrieve NDVI data.

As a response to the methodological and economic challenges with passive sensors and field spectrometers, low-cost active crop canopy sensors, equipped with their own light sources, have been developed during the last two decades, instantaneously providing an NDVI reading within a second (Rutto and Arnall 2017; Aranguren et al., 2020). Such devices, originally developed for precision agriculture, are not limited by ambient light conditions, which allow for consistent and accurate monitoring of NDVI from vegetated plots or individual plants (Anderson et al., 2016; Bjerke et al., 2017; Lu et al., 2017). However, to our knowledge, active NDVI sensors have rarely been applied on lichen-dominated plots; Barták et al. (2015, 2016, 2018, 2021), and Orekhova et al. (2018) used an active sensor (“PlantPen NDVI 300”, Photon System Instruments, Czech Republic) to study NDVI changes in single lichen thalli during dehydration processes or artificial removal of acetone-soluble UV-absorbing pigments. In Table 1, we present typical NDVI values for vascular plants, bryophytes, biocrusts and soil measured by active sensors in previous studies from boreal and arctic regions.

However, it remains unknown how lichen cover affects active-sensor NDVI values and how these numbers correlate with values from passive sensors such as satellites, leaving us in the dark regarding the applicability of handheld sensors to monitor lichen abundance, and the possibility to link field measurements to satellite-based remote sensing. There is considerable physical variation among lichen species, thus we focused our study on pale, fruticose lichens. Those are the ecologically, economically and culturally most important species in our research area, as they constitute by far the largest biomass, and are an important food resource for wild and domestic reindeer (*Rangifer tarandus*) (Tømmervik et al., 2012; Riseth et al., 2016). In addition to their biological importance, they may, if abundant, also affect local climate due to higher albedo (Stoy et al., 2012).

The objectives of this study are hence (1) to assess the feasibility of active handheld sensors to detect relationships between NDVI and pale lichen ground cover, and (2) to compare ground-based active sensor-NDVI values with measurements from the Sentinel-2 satellites in plots with varying lichen cover.

2. Methods

2.1. Study sites

We recorded NDVI in the field with active sensors in 3 study areas along a 2000 km latitudinal gradient from boreal and low-arctic heathlands in mainland Norway to high-arctic tundra in Svalbard (covering latitudes from 62° N to 79° N, Table 2, Fig. 1). The data were collected in 2018 and 2020.

2.2. Data collection

We measured NDVI manually at each field plot (1 m × 1 m, $n = 422$) with the Trimble *GreenSeeker Handheld Crop Sensor* HCS-100 (Trimble Westminster, CO, USA) (hereafter termed as ‘Greenseeker’). In 174 plots in Røros (Fig. 1), we also recorded NDVI with the RapidSCAN CS-45 (Holland Scientific, Lincoln, NE, USA; hereafter termed as ‘RapidSCAN’), parallel to the Greenseeker measurements. Both devices have light-emitting diodes for red (R: 670 nm) and near-infrared (NIR: 780 nm) light, both of which are required input data for the calculation of NDVI. The RapidSCAN device also incorporates an additional red-edge

Table 1

Published NDVI values for some common arctic and boreal plants and vegetation types using the active sensors “Greenseeker” and “RapidSCAN”. The table includes only measurements on healthy plants/vegetation types.

Species	NDVI range	Study site	n plots	References
Dwarf shrubs				
<i>Calluna vulgaris</i>	0.68–0.80	Lofoten, Troms, Norway	125	Bjerke et al., (2017)
<i>Cassiope tetragona</i>	0.58–0.61	Adventdalen, Svalbard	28	Anderson et al., 2016
<i>Dryas octopetala/ Salix polaris/ Biocrust</i>	0.30–0.40	Adventdalen, Svalbard	31	Anderson et al., (2016)
<i>Empetrum nigrum</i>	0.65–0.85	Lofoten, Troms, Norway	111	Bjerke et al., (2017)
<i>Empetrum nigrum</i>	0.65	Tromsø, Norway	59	Ritz et al., (2020)
Graminoid/ <i>Salix polaris</i>	0.50–0.56	Adventdalen, Svalbard	33	Anderson et al., (2016)
<i>Vaccinium myrtillus/Avenella flexuosa</i>	0.60–0.70	Røros	3	Tømmervik et al., (2021)
Graminoids				
<i>Luzula</i> sp.	0.48–0.52	Adventdalen, Svalbard	15	Anderson et al., (2016)
Graminoid/ bryophyte vegetation	0.60–0.63	Adventdalen, Svalbard	30	Anderson et al., (2016)
Bryophytes				
<i>Racomitrium</i> sp.	0.21–0.35	Svalbard	19	Finne, unpublished
<i>Racomitrium</i> sp.	0.33–0.34	East-Iceland	4	Óskarsdóttir et al., (2019),
Moss tundra	0.31–0.60	Svalbard, North Norway	15	Finne, unpublished
Lichens				
<i>Umbilicaria</i> Sp	0.10–0.60	Laboratory		Barták et al., (2015)
Mixed, 4 Antarctic, 2 Argentinian	0.23–0.57	Laboratory		Barták et al., (2016)
Mixed, 5 Antarctic	0.05–0.40	Laboratory		Barták et al., (2018)
Mixed, 4 Antarctic	0.16–0.37	Laboratory		Orekhova et al., (2018)
Mixed, 5 Antarctic	0.06–0.33	Laboratory		Barták et al., (2021)
Soil	0.05–0.20	High arctic		Walker et al., 2012*
Biological soil crust (wet)	0.32	Krenkel, Hayes island		Walker et al., 2012*
Biological soil crust (dry)	0.43–0.49	Krenkel, Hayes island		Walker et al., 2012*
Rock, stone	0.01–0.10			Finne unpublished

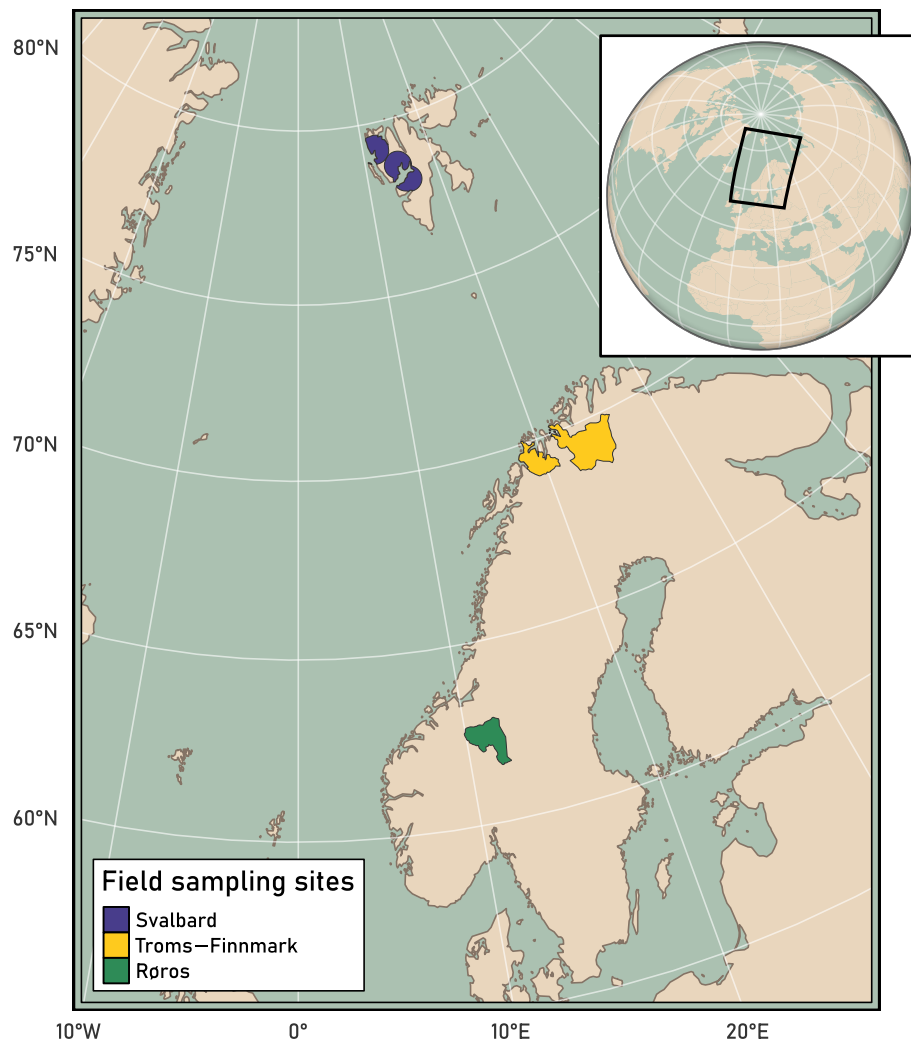
band (RE: 730 nm). When the sensor is activated, light is beamed onto the plant canopy of the target vegetation, and the reflected light, measured with silicon diodes, is used for the calculation of NDVI. The sensors can be operated at sensor-to-canopy distances ranging from 0.3 m to 3.0 m and are not affected by measurement height within that range (Lu et al., 2017). However, height affects the covered area. At the 1 m height used in our data collection, the sensor footprint of the Greenseeker can be approximated by an ellipse measuring 80 cm on the long axis and 30 cm on the short axis whereas the field of view of the RapidSCAN is approximately 80 × 20 cm (according to the documentation of the manufacturers).

The number of measurements from the 3 study sites (Fig. 1) are listed

Table 2

Summary of the study regions, including year, latitude, ecosystem type, dominant lichen species, and number of ground and satellite observations.

Region	Year	Latitude	Ecosystem	Dominant lichen species	n ground observations	n satellite observations
Svalbard	2020	78.6–79.3	High Arctic	<i>Cetrariella delisei</i> , <i>Cladonia mitis</i> , <i>Flavocetraria nivalis</i>	67	27
Finmark	2018	68.6–69.1	Sub-Arctic	<i>Cladonia arbuscula</i> , <i>Cladonia stellaris</i>	116	101
Troms-Finmark	2020	68.7–69.2	Sub-Arctic	<i>C. arbuscula</i> , <i>C. stellaris</i>	33	18
Røros	2020	61.7–62.7	Northern boreal	<i>C. stellaris</i> , <i>C. arbuscula</i>	209	204

**Fig. 1.** Map of the field sampling sites distributed between 62° and 79° N.

in Table 2. The NDVI measurements were acquired in two ways for each plot; one point measurement with the sensor directed towards the centre of the plot, and a sweep recording, where the instrument automatically averages multiple readings while being swept horizontally across a plot. The diagonal sweep measurements were used in all analyses except the correlation test between the two active sensors, where the centre point values were used since multiple sweep measurements from the RapidSCAN failed to be recorded.

2.3. Estimates of lichen cover

2.3.1. Digital photographic classification

We applied a digital photographic unsupervised isodata classification of field-plot photos following the methodology described first by Vanha-Majamaa et al. (2000), Sandström et al. (2003) and Tømmervik et al. (2012) for the 113 plots from Finnmark registered in 2018 (Table 2). The primary objective with this classification was to retrieve exact horizontal cover of the various vegetation groups and non-vegetated parts. The vegetation groups were pale fruticose lichens of the genera *Cladonia* and *Flavocetraria*, other lichens, moss, graminoids, and shrubs. We classified each digital field-plot photo using an

unsupervised ISODATA, automatic classification algorithm in the ENVI software provided by L3 Harris Geostpatial (Broomfield, Colorado). The percentage cover of the various vegetation groups was automatically calculated. All classes from the classification phase were interpreted using colour composites, field data (visual cover estimated), and other sources of information following the methodology applied by Sandström et al. (2003) and Tømmervik et al. (2012).

A limited number ($n = 53$) of randomly selected, digital classified images of the field plots from Finnmark in 2018, in which cover was also visually estimated in field, were used for assessment of accuracy (Scherrer and Pickering 2005; Tømmervik et al., 2012). For further control of this assessment, we ocularly compared the photos of the field plots with the classified field plot imagery, ($R^2 = 0.78$, $n = 53$, $p < 0.001$) in order to get comparable data with the field data from Svalbard and Troms-Finnmark. For the field plots in Svalbard ($n = 67$) and Troms-Finnmark 2020 ($n = 33$) we estimated the relative vascular plant cover ocularly from plot photos.

Since we were interested in comparing lichens with green plants, and rock has a much lower NDVI than green plants (Table 1), we removed all plots with $>10\%$ rock or stone cover prior to analysing.

2.3.2. Visual and plot-frame estimations

For the remaining 209 (Røros) plots, vegetation cover was estimated in the field by ocular estimation (percentage of the area within the $1\text{ m} \times 1\text{ m}$ plot) for the same vegetation groups. In addition to visual vegetation cover, we recorded species composition by point-intercept estimation using a quadrat frame on adjustable legs, elevated just above the tallest vegetation. Since the data collection was undertaken as part of several different monitoring programs, data rely on two different frames. In Finnmark in 2018, we used a $1\text{ m} \times 1\text{ m}$ frame with 100 intercept points. For all other sites, we used a frame that had a $0.3\text{ m} \times 0.3\text{ m}$ frame with 66 intercept points. A metal rod (5 mm diameter) held vertically was used to count hits at each intercept. If the rod hit rocks, soil, or animal droppings, these were also recorded. Vegetation was generally homogenous within each 1 m^2 plot, and the difference in point intercept frame size had no implications for the results since we only used the intercepts for species composition estimates.

Due to overlapping layers of certain lichen species, some observations of absolute cover exceeded 100%. In the analyses, however, we used relative cover, summing up to 100%.

2.4. Extraction of satellite NDVI (Sentinel-2)

To compare ground-based NDVI with satellite NDVI, we calculated NDVI for each coordinate based on Sentinel-2 satellite images ($10\text{ m} \times 10\text{ m}$ resolution, no plots appeared in the same pixel) from scenes acquired as close as possible in time to the ground measurements. We used Google Earth Engine (Gorelick et al., 2017) to access Level-2A Sentinel scenes and used the embedded cloud probability assessment (with a threshold of 5% chance) to mask clouds and cloud shadows. The RapidSCAN features a red-edge band, allowing for a comparison with satellite derived NDRE index. However, we did only have access to this device during the end of the field work, and the limited number of field plots did not call for a meaningful comparison with satellite values.

2.5. Statistical analysis

2.5.1. Active NDVI in relation to vegetation cover

To assess the effect of pale lichen cover (%) on the field NDVI measurements, we fitted 3 linear models with: a) only lichen cover, b) only vascular plant cover, and c) both lichen and vascular plant cover, as explanatory variables. The explanatory value of the candidate models were compared using Akaike information criterion (AIC).

As datapoints from the same areas could not be assumed to be independent from each other, we first fitted models with study area as a random factor. However, as the models with and without this random

factor turned out to be practically identical, we present the results of normal linear models, due to their simplicity.

We also compared measurements of the two handheld devices from 174 plots in the Røros area (Fig. 1). We fitted a linear model to compare the results from the sweep average values in each plot.

2.5.2. Active NDVI and satellite NDVI

When comparing the active NDVI measurements with the Sentinel-2 satellite values, we first did it separately for each area, fitting linear regression models with satellite NDVI as the response variable and active ground measured NDVI as explanatory variables. After determining that there were no differences between the slopes for the different areas, using Tukey post-hoc comparison, we also constructed a joint model for all areas.

Two possible approaches were assessed for comparison of field measurements with satellite-derived values. These were (1) to select satellite images that were as close in time to the field sampling as possible, or (2) to select images of the highest quality within a longer time frame (± 3 weeks). The potential advantage of the first approach is that a minor time difference minimizes any deviation caused by moisture, vegetation senescence, phenological events or other changes of the vegetation. However, the quality of the selected image might be limited if acquired during suboptimal atmospheric conditions. The second approach, which allows for selection of high-quality images, provides the most accurate NDVI measurement, but there is a risk for larger deviation with increasing time difference between the field-based and the satellite-based measurements.

Since we were able to obtain satellite images within a reasonable time frame (1–18 days), we opted for a hybrid between the two approaches. When multiple dates with high-quality images were available, we selected the images of the date that showed the highest correlation with the field data (Table 3, Figures S1A–D). By doing this, we avoided artificially inflated mismatches caused by undetected disturbances such as atmospheric noise. However, to rule out any potentially systematic effect of time difference, we tested if there was a relationship between the residuals of the final model and the date difference by fitting a linear model with time difference in days as explanatory variable and residuals from the correlation as response variable. All analyses were done in R version 4.0.3 (R Core Team, 2021) and primarily the packages: lme4 (v.1.1.26, Bates et al., 2015), sf (v. 1.0.4., Pebesma, 2018), tmap (v. 3.3.2, Tennekes, 2018).

3. Results

We collected data from 483 plots with pale lichen cover ranging from 0 to 100%. There was regional variation in species composition where *Flavocetraria nivalis* (syn. *Nephromopsis nivalis*) was most abundant in Svalbard and the Troms-Finnmark region, while *Cladonia stellaris* was most abundant in the Røros region (Fig. 1).

3.1. NDVI ground measurements in relation to vegetation cover

NDVI measured in the field was negatively correlated to pale lichen cover while it was positively related to vascular plant cover ($n = 422$, $p < 0.001$, $df = 1$, Table 3, Fig. 2). A comparison of the models showed that the model including both vascular plant cover and lichen cover as explanatory variables performed best (Table 3). The range of NDVI values for lichens appeared to be above 0.4 when the lichen cover was below 40%, whereas when lichen cover was between 40 and 100% the NDVI range was 0.4–0.18, thus decreasing with increasing lichen cover (Fig. 2). The pattern was similar for all areas, although natural variation in lichen abundance caused the range of sampled lichen cover to differ between study areas.

The parallel field measurements of the two sensors Greenseeker and RapidSCAN showed a positive relationship ($r = 0.79$, $p < 0.001$, Fig. S3).

Table 3

Comparison of the different candidate models with Greenseeker NDVI as response variable, and vascular plant and lichen cover as explanatory variables. The model combining both vascular plants and lichen cover performed best, as indicated by the lowest Akaike information criterion (AIC) score.

Explanatory variables	n			AIC		Coefficients		R ²
	vars	AIC	ΔAIC	Weight	Log likelihood	Lichen	Vascular	
Lichen + vascular cover	2	-913	0	1	461	-0.0015	0.0028	0.61
Vascular cover	1	-819	94.9	0	412	-	0.0039	0.52
Lichen cover	1	-732	181.7	0	369	-0.003	-	0.40

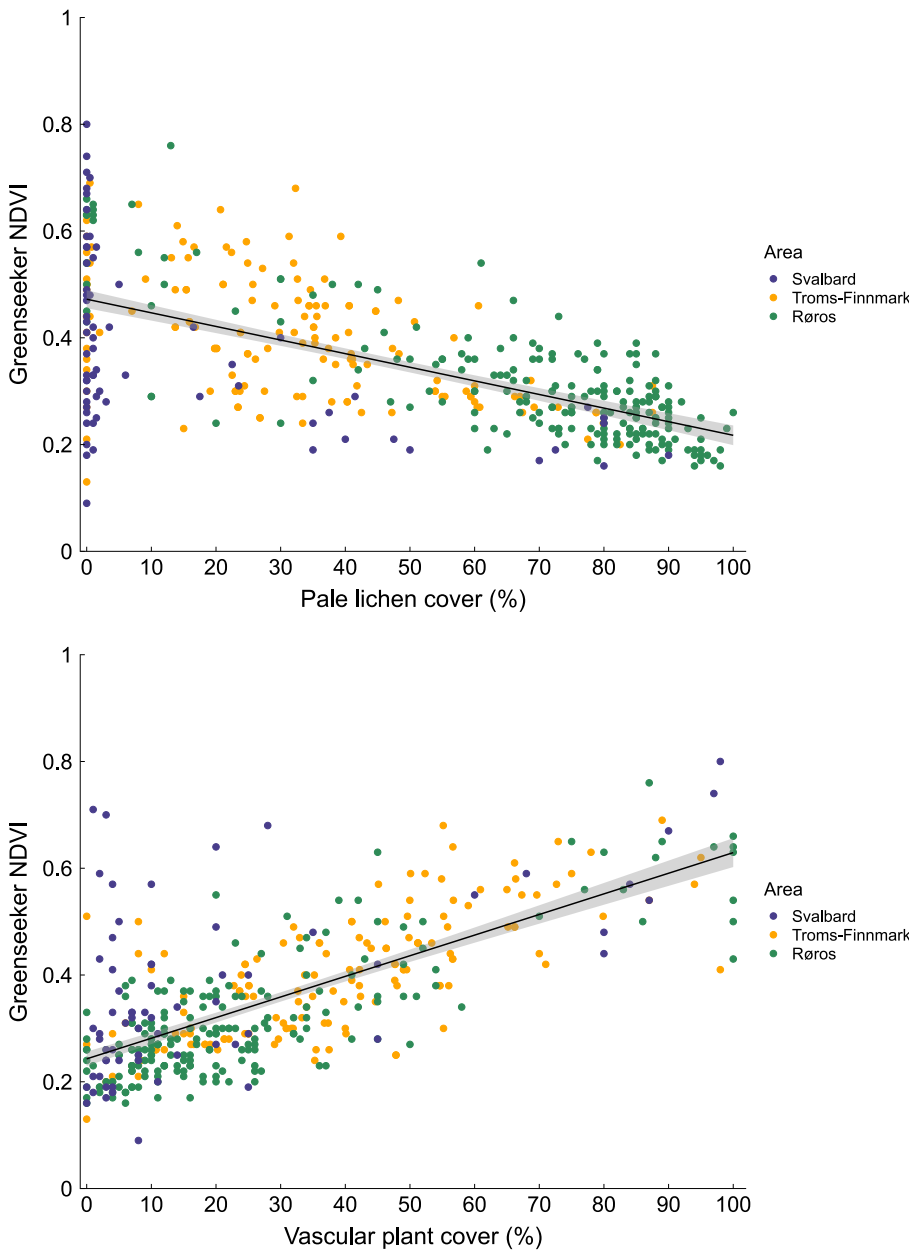


Fig. 2. Normalised Difference Vegetation Index (NDVI) measured with the handheld active sensor Greenseeker was negatively related to cover of pale lichens ($n = 422$, $df = 1$, $t = -10.4$, $SE = 0.00014$ $p < 0.001$, slope = -0.0015), while it was positively related to vascular plant cover ($n = 422$, $df = 1$, $t = 15.1$, $SE = 0.00019$, $p < 0.001$ slope = 0.0028). The shaded area indicates 95% confidence interval, calculated for each explanatory variable separately. The pattern was similar across all three study sites along a latitudinal gradient ranging from 62° N to 79° N. (Figures showing the relationship with satellite derived NDVI are included in the supplementary data, Fig. S2.)

3.2. Relationships between active NDVI and Sentinel-2 NDVI

The relationship (slope) between satellite and field active NDVI did not differ between the study areas (Tukey post-hoc pairwise comparison, $p > 0.6$ for all pairs), so we constructed a joint model for all regions (the separate correlations for each site and satellite image are shown in Fig. S4). Sentinel 2 and Greenseeker NDVI were positively correlated across all field sites ($n = 358$, $R = 0.61$ $p < 0.001$, Table 3). However, the

satellite values were generally higher, especially for lower NDVI values, and the slope of the joint model regression line was 0.54 with an intercept of 0.34 (Fig. 3). When analysed separately, Svalbard had the highest correlation with the field data ($R^2 = 0.81$) while the other sites were close to $R^2 = 0.30$ (Table 4).

The difference in time between satellite measurements and ground measurements posed a negligible effect on the NDVI relationships, as shown by low (negative) or no correlations between the residuals of the

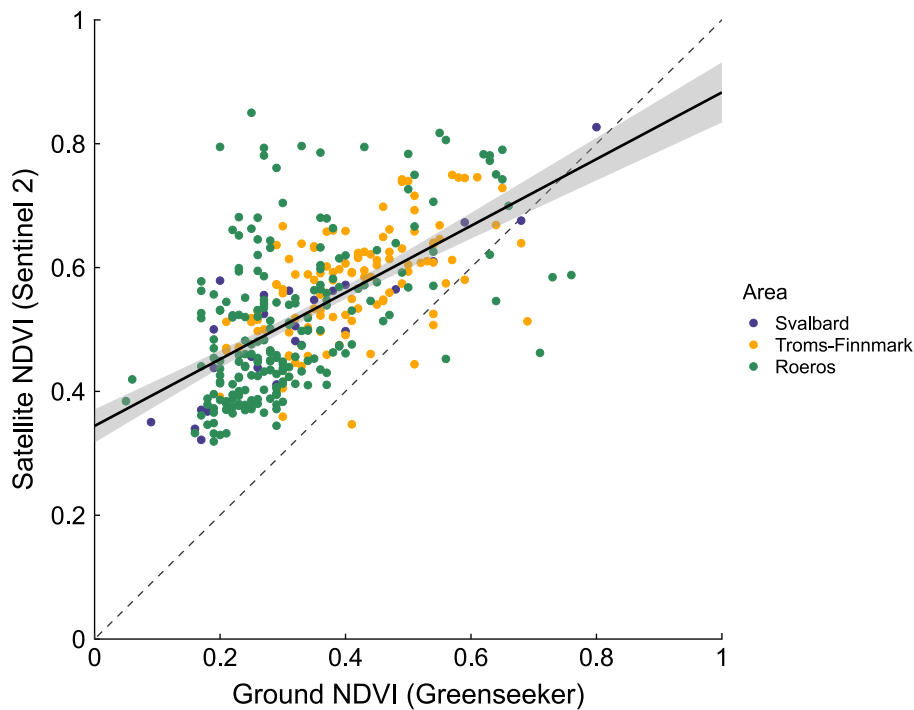


Fig. 3. Correlation between NDVI values from field-measurements using active sensor (Trimble Greenseeker) and the Sentinel 2 satellites ($n = 358$, $R = 0.61$, $df = 356$, $t = 14.56$, $SE = 0.037$, $p < 0.001$). Data were collected from three regions at different latitudes ranging from 62°N to 79°N. Predicted line of best fit from regression model (intercept = 0.34 ± 0.014 , slope = 0.54 ± 0.037) is shown in black with 95% CI. Dashed line indicates a 1:1 relationship as reference.

Table 4

Regional overview on relationships between NDVI from field measurements (Greenseeker) and derived NDVIs from satellite data (Sentinel-2). Date of ground measurements and satellite measurements, maximum difference in days between ground and satellite measurements, number of observations (n), correlations (r), and p -values for the correlations are included.

Site	Year	Date of ground measurements	Date of highest correlated satellite measurements	Days between measurements	R^2	n	p
Svalbard	2020	07.09–07.22	07.11	1	0.81	27	<0.01
Troms-Finnmark	2018	08.27–08.31	08.28	1	0.33	101	<0.01
Troms-Finnmark	2020	06.17–06.28	06.17	10	0.27	17	0.014
Røros	2020	08.18–09.20	09.02	18	0.29	213	<0.01

correlation analysis and the time difference (Troms-Finnmark: $R^2 = 0.11$, $p < 0.01$; Røros: $R^2 = 0.14$, $p < 0.01$; Svalbard: $R^2 = 0.01$, $p = 0.58$) (Fig. S5).

4. Discussion

We investigated the relationship between pale lichen cover and NDVI recorded with an active sensor in 422 field plots, from 3 study sites, ranging from boreal heath land to high arctic tundra. As expected, there was a positive relationship between vascular plant cover and NDVI. More notably, the relationship was inverted for lichens, as there was a negative relationship between lichen cover and NDVI. This was consistent across all study areas. Satellite NDVI was correlated with ground NDVI, but the relationship was not 1:1. Instead, satellite NDVI was consistently higher, especially for NDVI values below 0.5.

4.1. NDVI ground measurements in relation to lichen cover

Our data describes a transition from plots dominated by common types of boreal and tundra vegetation to plots dominated by lichens. Although there was considerable variation in NDVI values in the plots with no lichen cover, the general pattern was that lichens have lower NDVI than other boreal, alpine and arctic ground vegetation types. (A relationship that remained clear even when low lichen cover plots were removed from the analysis.) NDVI values reached as low as 0.2 in plots

with 80% or higher lichen cover. Our lichen values were lower than NDVI of tundra vegetation dominated by vascular plants and bryophytes measured by Anderson et al. (2016, Table 1), except plots dominated by a mixture of *Dryas octopetala* and *Salix polaris* that had NDVI between 0.30 and 0.40. Vegetation cover in those plots was however particularly patchy with biocrust or bare soil between the plants, and both species showed higher NDVI when mixed with other plants (Anderson et al., 2016). Bryophytes like *Racomitrium* spp. showed an overlap with lichens (Table 1). The effect of bare soil and biological soil crusts on NDVI is not uniform. While soil typically has NDVI values between 0.05 and 0.20 (Walker et al., 2012), biological soil crust varies a lot, but may have considerably higher values - reaching 0.4, especially when wet (Walker et al., 2012). An uneven mix of bare soil and biological soil crust is a likely explanation for the high variation in our NDVI measurements from Svalbard, where the vegetation cover was patchier and thinner than in the Norwegian mainland sites. However, our results suggest that pale lichens do have lower NDVI than other types of tundra vegetation and that handheld active NDVI sensors are useful for assessment of pale lichen cover and possibly also proximal biomass estimation.

In our analyses we grouped all pale lichen species together as the collected data did not allow for any analysis of specific lichen species. However, variation in lichen species composition and abundance between plots and regions could have added variation in NDVI as different lichen species have different reflective properties as shown experimentally in other studies (Kuusinen et al., 2020). In particular, a spectral

band placed in the SWIR area could potentially render a higher detection of total lichen cover and potentially biomass and differentiation of lichen species (Rees et al., 2004; Falldorf et al., 2014). The red-edge band (739 nm) of the RapidSCAN active sensor (which is similar to the spectral band 6 of Sentinel 2AB) may be a useful tool for rapid in-field cover detection of lichens, and hence, also useful in bio-monitoring programmes (Tømmervik et al., 1997; Zagajewski et al., 2017, 2018). In this study, we only had access to a RapidSCAN device during the last part of fieldwork in 2020, and further measurements and tests would be required for assessing its utility in lichen research and monitoring, particularly the potential benefits of the red-edge band. Our correlation test shows that there was some deviation in the NDVI values of the Greenseeker and the RapidSCAN devices. However, the deviation was smallest at lower NDVI values, indicating that the two devices produced similar results for lichen-dominated vegetation. However, further comparative measurements of lichen vegetation of different status and species composition would show if the red-edge band could provide a valuable new tool for detection of different species or stress.

4.2. Relationship between active ground-based measurements and spaceborne sentinel 2 measurements of NDVI

We were able to acquire clear satellite images taken relatively shortly before or after the field measurements. Since we found no or negligible effects of time lag on the correlation between satellite and field measurements, and since lichen-dominated vegetation is less influenced by phenology than vascular plant-dominated vegetation (Kershaw 1985; Nordberg and Allard 2002, May et al., 2017), we believe that our method for selection of satellite images worked well.

In general, satellite NDVI was higher compared to the ground-based active NDVI measurements, especially for values below 0.5. This result is expected since vegetation in the studied 1 m × 1 m plots in general was more homogenous than the vegetation cover on the 10 m × 10 m scale that Sentinel-2 NDVI-values are calculated from. Especially in plots dominated by lichens and with no or little green vegetation, our experience from the field suggests that the surrounding area generally encompassed more green vegetation. Even in areas with thick lichen cover, patches of green plants usually occurred, either as mat-forming evergreens, or as protruding graminoids, sporadic clusters of forbs and shrubs shading lichens that were growing underneath them. A similar but even stronger effect applies to boreal plots in Troms-Finnmark and Røros where lichen heath is dominant between scattered individual trees – or clusters of trees, primarily Scots pine (*Pinus sylvestris*) and birch (*Betula pubescens*) (Tømmervik et al., 2012). In these situations, the tree canopy significantly increased satellite NDVI compared to the NDVI values of the surrounding field and bottom layers, i.e., the short vegetation characterized by dwarf shrubs, graminoids, bryophytes and lichens (Peltoniemi et al., 2005; Rautiainen et al., 2007; Forsström et al., 2019).

The general relationship between satellite and ground NDVI was similar between regions, but the correlations were much weaker at Røros and Troms-Finnmark ($R^2 \approx 0.3$) than on Svalbard ($R^2 \approx 0.8$). A possible reason for this is that the sparse high-arctic vegetation on Svalbard is not mixed with tree and shrub layers. Thus, a single 1 m² plot in a plane area of the high-Arctic is more likely to be representative for the larger 100 m² area surrounding it than a single 1 m² plot in boreal or low-arctic regions where taller vegetation is more likely to partly shade the ground layer. Additionally, vegetation moisture levels might also vary between the high-Arctic and the boreal and low-Arctic regions, as Svalbard receives much less precipitation than the wetter areas of Troms-Finnmark and Røros (Grinde et al., 2021). Another reason could be that morning and midday dew (Lakatos et al., 2012; Proctor 2012) resulting in a wetter lichen surface in the first part of the day in the boreal region like Røros, hence reducing the relationship between satellite and ground measurements of NDVI. Finally, lower frequency of hazy conditions in high-Arctic Svalbard can improve the relationship

between satellite and ground-based measurements, compared with areas further south (Myers-Smith et al., 2020).

The generally low NDVI associated with high lichen cover, in combination with the in general higher NDVI values derived from Sentinel 2, suggests that satellites, at least with the 10 m × 10 m and coarser resolutions, may be suboptimal as a stand-alone solution for remote sensing of lichen cover. For example, a combination of sparse green vegetation and bare soil can approach similar NDVI as a dense pale lichen cover. However, since our sampling method was primarily designed to evaluate the hand-held devices, and not to fit 10 × 10 m resolution, our results are not a rigorous test of the suitability of the Sentinel satellites for remote sensing of lichens. Imagery acquired by other platforms such as drones, aircrafts and satellites with sensors that have very high spatial resolution will probably fit more directly with NDVI-measurements done by active sensors like Greenseeker and RapidSCAN.

5. Conclusions

In this study we have shown that NDVI values acquired with two different types of active NDVI sensors decreased with increasing cover of pale lichens in three different lichen-dominated areas distributed from the middle boreal region in Mid-Norway to the high-Arctic region on Svalbard. Ground-based NDVI explained more of the variation in satellite NDVI in the high-Arctic ($R^2 = 0.81$) than in boreal and lower-Arctic regions, likely due to tree and shrub canopy effects in the latter regions ($R^2 = 0.30$). While NDVI is highly sensitive to plant senescence and phenology, lichens have a more constant NDVI value throughout the growing season, even though values might vary with moisture levels and species composition. This indicates a clear potential applicability of active NDVI sensors in estimation of lichen coverage, and further development of ground-based methods assessing lichen status will be an attractive and useful addition to the many applications of NDVI in vegetation monitoring. The method could be readily used as a convenient and low-cost addition to high-latitude vegetation monitoring applications, possibly combined with high-resolution satellite NDVI in areas with no, or little, tree cover.

Author's contribution statements

HT conceived the idea. EAF, HT, JWB, MKA, RE planned and carried out the fieldwork. MKA, RE analysed the data. MKA, RE took the lead in writing the manuscript. All authors actively discussed the results and participated in the writing of the manuscript.

Declaration of competing interest

None.

Acknowledgements

HT, MKA, RE, LN, EAF and JWB received financial support from the Research Council of Norway (projects 287402 (VANWHITE) and 294948 (EMERALD)), and from FRAM–High North Research Centre for Climate and the Environment through its terrestrial flagship program (projects 369910 and 369924).

Appendix A. Supplementary data

Supplementary data to this article can be found online at <https://doi.org/10.1016/j.funeco.2023.101233>.

References

- Anderson, H.B., Nilsen, L., Tømmervik, H., Karlsen, S.R., Nagai, S., Cooper, E.J., 2016. Using ordinary digital cameras in place of near-infrared sensors to derive vegetation indices for phenology studies of high arctic vegetation. *Rem. Sens.* 8, 847. <https://doi.org/10.3390/rs8100847>.

- Aranguren, M., Castellón, A., Aizpurua, A., 2020. Wheat yield estimation with NDVI values using a proximal sensing tool. *Rem. Sens.* 12, 2749. <https://doi.org/10.3390/rs12172749>.
- Barták, M., Hájek, J., Amarillo, A.C., Hazdrová, J., Carreras, H., 2016. Changes in spectral reflectance of selected Antarctic and South American lichens caused by dehydration and artificially-induced absence of secondary compounds. *Czech Polar Reports* 6, 221–230. <https://doi.org/10.5817/CPR2016-2-20>.
- Barták, M., Hájek, J., Morkusová, J., Skácelová, K., Košuthová, A., 2018. Dehydration-induced changes in spectral reflectance indices and chlorophyll fluorescence of Antarctic lichens with different thallus color, and intrathalline photobiont. *Acta Physiol. Plant.* 40, 177. <https://doi.org/10.1007/s11738-018-2751-3>.
- Barták, M., Hájek, J., Orekhova, A., Villagra, J., Marín, C., Palfner, G., Casanova-Katny, A., 2021. Inhibition of primary photosynthesis in desiccating Antarctic lichens differing in their photobionts, thallus morphology, and spectral properties. *Microorganisms* 9, 818. <https://doi.org/10.3390/microorganisms9040818>.
- Barták, M., Trnková, K., Hansen, E.S., Hazdrová, J., Skácelová, K., Hájek, J., Forbelská, M., 2015. Effect of dehydration on spectral reflectance and photosynthetic efficiency in *Umbilicaria arctica* and *U. hyperborea*. *Biol. Plant.* (Prague) 59, 357–365. <https://doi.org/10.1007/s10535-015-0506-1>.
- Bates, D., Maechler, M., Bolker, B., Walker, S., 2015. Fitting linear mixed-effects models using lme4. *J. Stat. Software* 67 (1), 1–48. <https://doi.org/10.18637/jss.v067.i01>.
- Bjerke, J.W., Treharne, R., Vikhamar-Schuler, D., Karlsen, S.R., Ravolainen, V., Bokhorst, S., Phoenix, G.K., Bochenek, Z., Tømmervik, H., 2017. Understanding the drivers of extensive plant damage in boreal and Arctic ecosystems: insights from field surveys in the aftermath of damage. *Sci. Total Environ.* 599–600. <https://doi.org/10.1016/j.scitotenv.2017.05.050>, 1965–1976.
- Blunden, J., Boyer, T., 2021. State of the climate in the 2020. *Bull. Am. Meteorol. Soc.* 102, S1–S475. <https://doi.org/10.1175/2021BAMSStateoftheClimate.1>.
- Bokhorst, S., Tømmervik, H., Callaghan, T.V., Phoenix, G.K., Bjerke, J.W., 2012. Vegetation recovery following extreme winter warming events in the sub-Arctic estimated using NDVI from remote sensing and handheld passive proximal sensors. *Environ. Exp. Bot.* 81, 18–25. <https://doi.org/10.1016/j.envexpbot.2012.02.011>.
- Brodo, I.M., Sharnoff, S.D., Sharnoff, S., 2001. *Lichens of North America*. Yale University Press.
- Chagnon, C., Simard, M., Boudreau, S., 2021. Patterns and determinants of lichen abundance and diversity across a subarctic to arctic latitudinal gradient. *J. Biogeogr.* 48, 2742–2754. <https://doi.org/10.1111/jbi.14233>.
- Edwards, M., Henry, G.H.R., 2016. The effects of long-term experimental warming on the structure of three High Arctic plant communities. *J. Veg. Sci.* 27, 904–913. <https://doi.org/10.1111/jvs.12417>.
- Erlandsson, R., Bjerke, J.W., Finne, E.A., Myneni, R.B., Piao, S., Wang, X., Virtanen, T., Räsänen, A., Kumpula, T., Kolari, T.H.M., Tahvanainen, T., Tømmervik, H., 2022. An artificial intelligence approach to remotely assess pale lichen biomass. *Remote Sens. Environ.* 280, 113201. <https://doi.org/10.1016/j.rse.2022.113201>.
- Falldorf, T., Strand, O., Panzacchi, M., Tømmervik, H., 2014. Estimating lichen volume and reindeer winter pasture quality from Landsat imagery. *Remote Sens. Environ.* 140, 573–579. <https://doi.org/10.1016/j.rse.2013.09.027>.
- Forsström, P., Peltoniemi, J., Rautiainen, M., 2019. Seasonal dynamics of lingonberry and blueberry spectra. *Silva Fenn.* 53, 10150. <https://doi.org/10.14214/sf.10150>.
- Fraser, R.H., Lantz, T.C., Olthof, I., Kokelj, S.V., Sims, R.A., 2014. Warming-induced shrub expansion and lichen decline in the western Canadian arctic. *Ecosystems* 17, 1151–1168. <https://doi.org/10.1007/s10021-014-9783-3>.
- Gamon, J.A., Huemmrich, K.F., Stone, R.S., Tweedie, C.E., 2013. Spatial and temporal variation in primary productivity (NDVI) of coastal Alaskan tundra: decreased vegetation growth following earlier snowmelt. *Remote Sens. Environ.* 129, 144–153. <https://doi.org/10.1016/j.rse.2012.10.030>.
- Gorelick, N., Hancher, M., Dixon, M., Ilyushchenko, S., Thau, D., Moore, R., 2017. Google earth engine: planetary-scale geospatial analysis for everyone. *Remote Sens. Environ.* 202, 18–27. <https://doi.org/10.1016/j.rse.2017.06.031>.
- Grinde, L., Heiberg, H., Kristiansen, S., Mamen, J., Skaland, R.G., Tilley Tajet, H.T., Tunheim, K., 2021. Været i Norge, Klimatologisk oversikt året 2021. *Meteorologisk institutt*, vol 13/2021, 1–28.
- Joly, K., Jandt, R.R., Klein, D.R., 2009. Decrease of lichens in Arctic ecosystems: the role of wildfire, caribou, reindeer, competition and climate in north-western Alaska. *Polar Res.* 28, 433–442. <https://doi.org/10.1111/j.1751-8369.2009.00113.x>.
- Kennedy, B., Pouliot, D., Manseau, M., Fraser, R., Duffe, J., Pasher, J., Chen, W., Olthof, I., 2020. Assessment of landsat-based terricolous macrolichen cover retrieval and change analysis over caribou ranges in northern Canada and Alaska. *Remote Sens. Environ.* 240, 111694. <https://doi.org/10.1016/j.rse.2020.111694>.
- Kershaw, K.A., 1985. *Physiological Ecology of Lichens*. Cambridge University Press, Cambridge, U.K.
- Kumpula, J., Kurkilahti, M., Helle, T., Colpaert, A., 2014. Both reindeer management and several other land use factors explain the reduction in ground lichens (*Cladonia* spp.) in pastures grazed by semi-domesticated reindeer in Finland. *Reg. Environ. Change* 14, 541–559. <https://doi.org/10.1007/s10113-013-0508-5>.
- Kuusinen, N., Juola, J., Karki, B., Stenroos, S., Rautiainen, M., 2020. A spectral analysis of common boreal ground lichen species. *Remote Sens. Environ.* 247, 111955. <https://doi.org/10.1016/j.rse.2020.111955>.
- Lakatos, M., Obregón, A., Büdel, B., Bendix, J., 2012. Midday dew—an overlooked factor enhancing photosynthetic activity of corticolous epiphytes in a wet tropical rain forest. *New Phytol.* 194, 245–253. <https://doi.org/10.1111/j.1469-8137.2011.04034.x>.
- Lu, J., Miao, Y., Shi, W., Li, J., Yuan, F., 2017. Evaluating different approaches to non-destructive nitrogen status diagnosis of rice using portable RapidSCAN active canopy sensor. *Sci. Rep.* 7, 14073. <https://doi.org/10.1038/s41598-017-14597-1>.
- May, J.L., Healey, N.C., Ahrends, H.E., Hollister, R.D., Tweedie, C.E., Welker, J.M., Gould, W.A., Oberbauer, S.F., 2017. Short-Term impacts of the air temperature on greening and senescence in alaskan arctic plant tundra habitats. *Rem. Sens.* 9, 1338. <https://doi.org/10.3390/rs9121338>.
- Myers-Smith, I.H., Kerby, J.T., Phoenix, G.K., Bjerke, J.W., Epstein, H.E., Assmann, J.J., John, C., Andreu-Hayles, L., Angers-Blondin, S., Beck, P.S.A., Berner, L.T., Bhatt, U. S., Bjorkman, A.D., Blok, D., Bryn, A., Christiansen, C.T., Cornelissen, J.H.C., Cunliffe, A.M., Elmendorf, S.C., Forbes, B.C., Goetz, S.J., Hollister, R.D., de Jong, R., Loranty, M.M., Macias-Fauria, M., Maseyk, K., Normand, S., Olofsson, J., Parker, T. C., Parmentier, F.-J.W., Post, E., Schaepman-Strub, G., Stordal, F., Sullivan, P.F., Thomas, H.J.D., Tømmervik, H., Treharne, R., Tweedie, C.E., Walker, D.A., Wilkming, M., Wipf, S., 2020. Complexity revealed in the greening of the Arctic. *Nat. Clim. Change* 10, 106–117. <https://doi.org/10.1038/s41558-019-0688-1>.
- Myneni, R.B., Keeling, C.D., Tucker, C.J., Asrar, G., Nemani, R.R., 1997. Increased plant growth in the northern high latitudes from 1981 to 1991. *Nature* 386, 698–702. <https://doi.org/10.1038/386698a0>.
- Nordberg, M.L., Allard, A., 2002. A remote sensing methodology for monitoring lichen cover. *Can. J. Rem. Sens.* 28, 262–274. <https://doi.org/10.5589/m02-026>.
- Orekhova, A., Marečková, M., Hazdrová, J., Barták, M., 2018. The effect of upper cortex absence on spectral reflectance indices in Antarctic lichens during thallus dehydration. *Czech Polar Reports* 8, 107–118.
- Óskarsdóttir, G., Guðmundsdóttir, E., Ágústsdóttir, K., Tømmervik, H., 2019. Reindeer Winter Forage. Long-Term Monitoring Research (Work Carried Out for Landsvirkjun No. NA-190194). Náttúrustofa Austurlands, Iceland.
- Pebesma, E., 2018. Simple features for R: standardized support for spatial vector data. *R J.* 10 (1), 439–446. <https://doi.org/10.32614/RJ-2018-009>.
- Peltoniemi, J.I., Kaasalainen, S., Naranen, J., Rautiainen, M., Stenberg, P., Smolander, H., Smolander, S., Voipio, P., 2005. BRDF measurement of understory vegetation in pine forests: dwarf shrubs, lichen, and moss. *Remote Sens. Environ.* 94, 343–354. <https://doi.org/10.1016/j.rse.2004.10.009>.
- Piao, S., Wang, X., Park, T., Chen, C., Lian, X., He, Y., Bjerke, J.W., Chen, A., Ciais, P., Tømmervik, H., Nemani, R.R., Myneni, R.B., 2020. Characteristics, drivers and feedbacks of global greening. *Nat. Rev. Earth Environ.* 1, 14–27. <https://doi.org/10.1038/s43017-019-0001-x>.
- Proctor, M.C., 2012. Dew, where and when? There are more things in heaven and earth, Horatio, than are dreamt of in your philosophy.... *New Phytol.* 194, 10–11. <https://doi.org/10.1111/j.1469-8137.2012.04082.x>.
- R Core Team, 2021. *R: A Language and Environment for Statistical Computing*. R Foundation for Statistical Computing, Vienna, Austria.
- Rautiainen, M., Suomalainen, J., Mottus, M., Stenberg, P., Voipio, P., Peltoniemi, J., Manninen, T., 2007. Coupling forest canopy and understory reflectance in the Arctic latitudes of Finland. *Remote Sens. Environ.* 110, 332–343. <https://doi.org/10.1016/j.rse.2007.03.002>.
- Rees, W.G., Tutubalina, O.V., Golubeva, E.I., 2004. Reflectance spectra of subarctic lichens between 400 and 2400 nm. *Remote Sens. Environ.* 90, 281–292. <https://doi.org/10.1016/j.rse.2003.12.009>.
- Riseth, J.Å., Tømmervik, H., Bjerke, J.W., 2016. 175 years of adaptation: north Scandinavian Sámi reindeer herding between government policies and winter climate variability (1835–2010). *J. For. Econ.* 24, 186–204.
- Ritz, E., Bjerke, J.W., Tømmervik, H., 2020. Monitoring winter stress vulnerability of high-latitude understory vegetation using intraspecific trait variability and remote sensing approaches. *Sensors* 20, 2102. <https://doi.org/10.3390/s20072102>.
- Rouse, J.W., Haas, R.H., Deering, D.W., Schell, J.A., Harlan, J.C., 1974. *Monitoring the Vernal Advancement and Retrogradation of Natural Vegetation*. NASAGSFC Type III Final Rep. Greenbelt MD, p. 371.
- Rutto, E., Arnall, D.B., 2017. The history of the GreenSeeker™ sensor. In: *Oklahoma Cooperative Extension Fact Sheets*. Oklahoma State University, Stillwater, Oklahoma.
- Sandström, P., Granqvist Pahlén, T., Edenius, L., Tømmervik, H., Hagner, O., Hemberg, L., Olsson, H., Baer, K., Stenlund, T., Göran Brandt, L., Egberth, M., 2003. Conflict resolution by participatory management: remote sensing and GIS as tools for communicating land-use needs for reindeer herding in northern Sweden. *AMBIO A J. Hum. Environ.* 32, 557–567. <https://doi.org/10.1579/0044-7447-32.8.557>.
- Sandström, P., Cory, N., Svensson, J., Hedenas, H., Jougda, L., Borchert, N., 2016. On the decline of ground lichen forests in the Swedish boreal landscape: implications for reindeer husbandry and sustainable forest management. *Ambio* 45, 415–429. <https://doi.org/10.1007/s13280-015-0759-0>.
- Scherrer, P., Pickering, C.M., 2005. Recovery of alpine vegetation from grazing and drought: data from long-term photoquadrats in kosciuszko national park, Australia. *Arctic Antarct. Alpine Res.* 37, 574–584. [https://doi.org/10.1657/1523-0430\(2005\)037\[0574:ROAVFG\]2.0.CO;2](https://doi.org/10.1657/1523-0430(2005)037[0574:ROAVFG]2.0.CO;2).
- Serreze, M.C., Barry, R.G., 2011. Processes and impacts of Arctic amplification: a research synthesis. *Global Planet. Change* 77, 85–96. <https://doi.org/10.1016/j.gloplacha.2011.03.004>.
- Solheim, I., 1998. Bidirectional and Spectral Reflectance Properties of the *Cladonia Stellaris* and *Flavocetraria Nivalis* Lichens and the *Racomitrium Lanuginosum* Moss (Doctor Scientiarum Thesis). Tromsø University, Tromsø, Norway.
- Stoy, P.C., Street, L.E., Johnson, A.V., Prieto-Blanco, A., Ewing, S.A., 2012. Temperature, heat flux, and reflectance of common subarctic mosses and lichens under field conditions: might changes to community composition impact climate-relevant surface fluxes? *Arctic Antarct. Alpine Res.* 44, 500–508.
- Tennekes, M., 2018. Tmap: thematic maps in R. *J. Stat. Software* 84 (6), 1–39. <https://doi.org/10.18637/jss.v084.i06>.
- Tucker, C.J., 1979. Red and photographic infrared linear combinations for monitoring vegetation. *Remote Sens. Environ.* 8, 127–150. [https://doi.org/10.1016/0034-4257\(79\)90013-0](https://doi.org/10.1016/0034-4257(79)90013-0).

- Tømmervik, H., Johansen, B., Lauknes, I., 1997. Use of airborne laser spatial mode data for mapping of sub-arctic mountain heaths in pasvik, northern Norway. *Can. J. Rem. Sens.* 23, 230–242. <https://doi.org/10.1080/07038992.1997.10855205>.
- Tømmervik, H., Bjerke, J.W., Gaare, E., Johansen, B., Thannheiser, D., 2012. Rapid recovery of recently overexploited winter grazing pastures for reindeer in northern Norway. *Fungal Ecol., Fungi and Global Change* 5, 3–15. <https://doi.org/10.1016/j.funeco.2011.08.002>.
- Tømmervik, H., Erlandsson, R., Arneberg, M.K., Finne, E.A., Bjerke, J.W., 2021. Satellite Based Mapping of Winter Grazing Areas in Fæmund Sijte, Sålekinna-Håmmålsfjellet and Korssjøen-Feragen-Vest. (No. 1946), NINA Report. Norwegian Institute for Nature Research, Tromsø, Norway.
- Vanha-Majamaa, I., Salemaa, M., Tuominen, S., Mikkola, K., 2000. Digitized photographs in vegetation analysis - a comparison of cover estimates. *Appl. Veg. Sci.* 3, 89–94. <https://doi.org/10.2307/1478922>.
- Walker, D.A., Epstein, H.E., Raynolds, M.K., Kuss, P., Kopecky, M.A., Frost, G.V., Daniels, F.J.A., Leibman, M.O., Moskalenko, N.G., Matyshak, G.V., Khitun, O.V., Khomutov, A.V., Forbes, B.C., Bhatt, U.S., Kade, A.N., Vonlanthen, C.M., Tichy, L., 2012. Environment, vegetation and greenness (NDVI) along the north America and Eurasia arctic transects. *Environ. Res. Lett.* 7, 015504 <https://doi.org/10.1088/1748-9326/7/1/015504>.
- Zagajewski, B., Tømmervik, H., Bjerke, J.W., Raczko, E., Bochenek, Z., Klos, A., Jarocińska, A., Lavender, S., Ziolkowski, D., 2017. Intraspecific differences in spectral reflectance curves as indicators of reduced vitality in high-arctic plants. *Rem. Sens.* 9, 1289. <https://doi.org/10.3390/rs9121289>.
- Zagajewski, B., Kycko, M., Tømmervik, H., Bochenek, Z., Wojtuń, B., Bjerke, J.W., Klos, A., 2018. Feasibility of hyperspectral vegetation indices for the detection of chlorophyll concentration in three high Arctic plants: *Salix polaris*, *Bistorta vivipara*, and *Dryas octopetala*. *Acta Soc. Bot. Pol.* 87, 3604. <https://doi.org/10.5586/asbp.3604>.

Online references

- GreenSeeker Handheld Crop Sensor. n.d. URL. <http://www.trimble.com/Agriculture/gs-handheld.aspx> (accessed 3.9.21).
- RapidSCAN Cs\S-45. User's guide, n.d. URL. <https://hollandscientific.com/portfolio/rapidscan-cs-45/> (accessed 3.9.21).